Proceedings of 23rd International Scientific Conference. Transport Means 2019.

The Formation of Car Skid at a Safe Speed by Reducing the Radial Response of Car Wheels

P. Jilek[1], I. Sefčík[2], O. Voltr [3], J. Němec[4]

[1]*University of Pardubice, Studentská 95, 53210, Pardubuce, Czech Republic, E-mail: petr.jilek@upce.cz*
[2]*University of Pardubice, Studentská 95, 53210, Pardubuce, Czech Republic, E-mail: ivo.sefcik@upce.cz*
[3]*University of Pardubice, Studentská 95, 53210, Pardubuce, Czech Republic, E-mail: nemec.jan@upce.cz*

Abstract

The paper deals with the possibility of bringing a car to a skid level at a safe speed. Skid level is caused by a reduction in the adhesion force on car wheels by a decrease in radial responses on car wheels. The aim of the paper is to compare the behavioural changes of the experimental car with the sliding frame system against the driving of the experimental car on a sliding surface. In the work we deal with the analogy of the commercially available SkidCar system. Since the SC system is only produced for selected series-produced cars, we have designed a simplified version called Alternative SkidCar. It is an additional frame with four support wheels attached to the car. The mechanical movement of the support wheels affects the radial reaction transmitted by the car wheels. Car skid at a lower speed is caused by a reduction in adhesion force. To reduce the adhesion force transmitted by the car wheels, we transferred some of the radial response of the car wheel by means of additional support wheels. During the elaboration of the paper, we conducted experimental measurements which we compared with each other. As a test drive, we chose to drive the vehicle between cones, the so-called slalom test. The sliding surface was modified when constructing a test corridor for the Alternative SkidCar system. Since the Alternative SkidCar extends beyond the car's body, we had to adjust the corridor assembly to the sliding surface for this purpose. It can be seen from the evaluation of the measured waveforms that the Alternative SkidCar system can be used to change the adhesion force transmitted by the car wheels. The weight of the ASC frame reaches ¼ of the kerb weight, so the resulting measured characteristics are slightly different but still applicable. The results, collected during the experimental test, are presented and discussed. The Alternative SkidCar is used in the field as a primary tool to validate newly developed automotive electronic systems and to improve road safety in driver training. The Alternative SkidCar system helps to create any kind of skid relative to the longitudinal and lateral planes of the car.
KEY WORDS: *road vehicle, tires, adhesion, SkidCar*

1. Introduction

More and more emphasis is now put on autonomous driving. The car needs to be complemented with a range of electronic systems for autonomous driving. It is precisely for the development of these systems that considerable financial resources are spent. At the same time, these systems need to be tested for their proper operation and durability [4]. The testing process needs to be complemented by continuous monitoring of all car electronic systems [8]. Systems that help maintain car stability are important elements for road safety. Skid occurs when the car stability is impaired. The speed at which the skid is caused is determined by the car structure, tyre condition, adhesion properties, driving style and car weight parameters [9] and, last but not least, by maintenance [3, 10, 12]. Therefore, cars are tested primarily for lateral stability, i.e., lateral skid resistance. Real conditions are ideal for testing purposes, but it is not always possible to use these conditions. The results, collected during the experimental test, are presented and discussed. The development of the rear axle wheel turning system as an alternative to the commercially available ESP system is being prepared by the authors of the paper in their workplace. From this point of view, we were faced with the question of under what conditions to carry out the experiment. Given the initial design of the new system, we took the opportunity of using model conditions. The change in adhesion force can be achieved by reducing the coefficient of adhesion by using special tyres [1, 2] or special surface [7, 11]. The second option to reduce the adhesion force between the car wheel and the road is to reduce the radial response on the car wheels. This reduction can be achieved with the help of additional wheels. This system is called SkidCar in the commercial sector.

The authors' workplace has a unique experimental car that allows changing the direction of driving by turning the wheels of both axles. We are currently developing a system that will act as an alternative to the current ESP system by turning the rear axle wheels. To do this, we had to provide a methodology for how to bring a car to skid when driving 'safely'.

2. Materials and Methods

Commercially sold SkidCar is a device that consists of a supporting frame, a hydraulic circuit and an electronic steering system. The frame is always made for a specific car type and cannot be used on any other car. Because the rear

axle steering system is implemented on an individual construction of an experimental car, we made a parallel of the commercial SkidCar. The additional frame is attached to the body of the experimental car. We placed the crossbar with the front wheel units behind the front axle axis, the rear crossbar with wheel units in front of the rear axle axis. The location is intentional so that the car body can be more easily tilt in the longitudinal direction. The change of the radial reaction transmitted by the car wheels is set prior to the experimental measurement by mechanical ejection of the wheel unit. Based on the above-mentioned differences of our system from the commercially available SkidCar, we call our system Alternative SkidCar (ASC); Fig. 1.

Fig. 1 The experimental car with the alternative SkidCar system

Due to the fact that the ASC frame is sufficiently rigid, all body movements are based on the ACS wheel unit's flexibility. Thus, they are determined by the radial flexibility of the additional wheel tyres. The deformation characteristics of the support unit tyres were determined in static adhesor; see Fig. 2. The determination was based on a gradual loading with a vertical force. We always read the radial deformation from the position of the static adhesor arm at a specific load. Since we loaded the wheel from above through the tyre and not on the wheel axis, we divided the resulting deformation by two. The deformation characteristic is shown in Fig. 3 and is described according to (1) at a confidence interval of $R^2 = 0.9996$. There is increased noise emitted due to the rolling of additional ASC wheels; it is described in more detail [6].

$$y = -0.3441x^2 + 5.8352x\,. \tag{1}$$

Fig. 2 Determination of deformation characteristics of wheel units on static adhesor

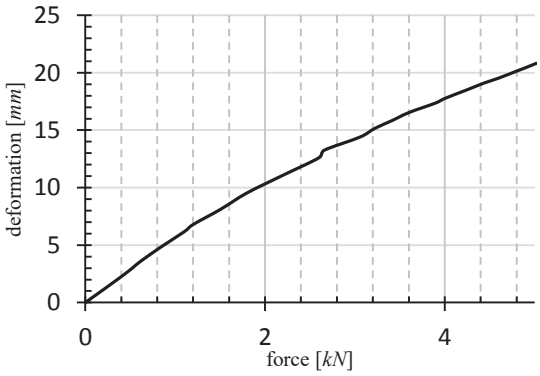

Fig. 3 Deformation characteristics of Alternative SkidCar wheel units

V The main car parameters changed due to the use of the Alternative SkidCar system. The outer width of the car increased by 845 mm to 2280 mm and the kerb weight increased by 198 kg to 1180 kg. The centre of gravity coordinates refer to the contact point of the left front wheel with the road. The centre of gravity coordinates in the longitudinal and lateral directions were determined using scales, and the height coordinate on the tilting platform (Table).

Table

Coordinates of car's centre of gravity

Weight and dimensional parameters	Experimental Car	Alternative SkidCar
Longitudinal coordinate of car's centre of gravity	T_x = 1335 *mm*	T_{SCx} = 1328 *mm*
Lateral coordinate of car's centre of gravity	T_y = 715 *mm*	T_{SCy} = 711 *mm*
Height coordinate of car's centre of gravity	T_z = 682 *mm*	T_{SCz} = 636 *mm*
Weight	m = 982 *kg*	m_{SC} = 1 198 *kg*

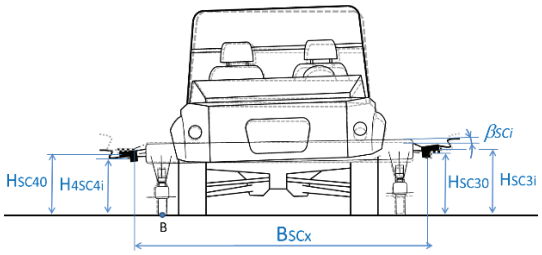

Fig. 4 Plane model of body cloning car with the ASC system

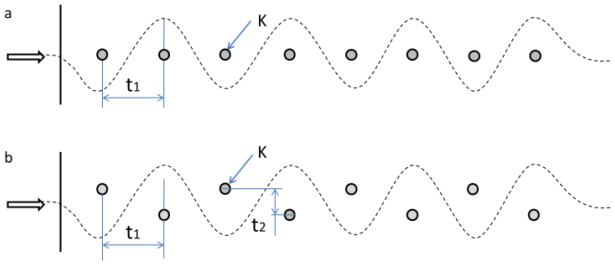

Fig. 5 Corridor for the slalom test: a – EX car, b – ASC, t_1 – distance between cones, K – cone, t_2 – cone offset

We selected the lateral skid of the car as a limit. Skid occurs when the lateral force is greater than the side force transmitted between the tyre and the road [5]. The size of the contact force is determined by the maximum adhesion force vector. The adhesion force can be reduced by changing the coefficient of adhesion or by changing the radial reaction, or both at the same time as shown in (2).

$$F_{ad_y} = \left(G \cdot \cos\beta + F_o \cdot \sin\beta\right) \cdot \varphi \,, \tag{2}$$

where F_{ad_y} – side force; F_o – centrifugal force, G – gravity of the vehicle; φ – coefficient of adhesion; β – slant slope of the road.

We used a slalom test drive to verify the behaviour of the car with the ASC system (Fig. 4). We compared the measured waveforms of the experimental car with the ASC system with the experimental car's drive on the sliding surface. The goal of the test is for the car to pass through a defined corridor between the cones at a predetermined speed. The speed at which the car has to pass through the corridor was obtained based on repeated experimental measurements on the sliding surface when we tried to drive through the corridor at a speed just before the skid. The design of the driving corridor is different for the sliding surface and the Alternative SkidCar. In the case of ASC, the cones (because of the ASC frame exceeding the car's body) had to be mutually reset by the increase in width, as shown in Fig. 5. We conducted the test drive for a 50% radial response on the car wheels. According to the manufacturer of the sliding surface, the coefficient of adhesion is 50% lower than that of dry asphalt.

We recorded the following quantities to monitor vehicle behaviour during the test drive. Speed v, slip angle φ and vehicle turning speed ω were measured using the Correvit sensor; lateral a_y and longitudinal a_x acceleration using two-axis acceleration sensor. The steering wheel turning angle β_v was measured indirectly using an analogue position sensor and calculated according to the relation (3) depending on the extension of the sensor cable wound on the steering column. The body tilt angle β_i was calculated from the signals of a pair of ultrasound distance sensors located at the place of the centre of gravity along the sides of the car.

$$\beta_{SCv} = \frac{180 \cdot l_{SCl}}{\pi \cdot r_{SCv}} - \beta_{SCvo} \,, \tag{3}$$

where β_{SCv} – actual steering angle; β_{SCv0} – steering angle for compensatory measurements; l_{SCl} – ejecting the sensor rope; r_{SCv} – radius of the steering shaft.

Before starting the experimental measurement in the set corridor, we first had to implement compensation measurement. This measurement is used to verify the functionality of the measuring chain and to obtain a set of compensation data. The compensation data set describes the initial state of the car, eliminates inaccuracies in sensor mounting and serves for off-time correction of measured waveforms. The compensation measurement also eliminates the initial state of body position when changing radial responses on the car wheels. The compensation measurement was performed in the form of ten repeated measurements at direct, steady drive in both directions on a 50m track. In this way, we obtained quasi-static waveforms of measured quantities for direct drive on a horizontal road (marked with index $_0$). We removed the remote values from the measured compensation measurements, which were obviously unrelated to the car's behaviour. Subsequently, we smoothened the measured waveforms using averaging. Thus, the values of longitudinal a_{x0} and lateral acceleration a_{y0}; the height coordinates of the left H_{SC30} and the right H_{SC40} part of the ASC frame; the height coordinates of the left H_{30} and the right H_{40} side of the body; the slip angle φ_0; the turning speed ω_0; and the steering wheel turning angle β_{vo} were obtained and used for the off-time correction of measured waveforms from the test drives.

The body tilt angle of the experimental car was calculated using relation (4), where H_{SC3i} (H_{SC4i}) is the vertical distance of the measuring point on the left (right) side of the ASC frame from the road at time t_i; B_{SCx} is the distance of the measuring points in the lateral plane of the ASC frame; H_{SC30} (H_{SC40}) is the distance of the measuring point on the left (right) side of the ASC frame from the road during the compensation measurements. The same applies accordingly to the experimental car on the sliding surface; the body tilt is determined according to relation (5). Where β_i is the body tilt angle; H_{3i} (H_{4i}) is the vertical distance of the sensor locations on the left (right) side of the body; B_x is the lateral distance of the measuring points on the body H_{30} (H_{40}) during the compensation measurements.

$$\beta_{SCi} = \tan^{-1}\left(\frac{\left(H_{SC3i} - H_{SC3o}\right) - \left(H_{SC4i} - H_{SC4o}\right)}{B_{SCx}}\right); \tag{4}$$

$$\beta_i = \tan^{-1}\left(\frac{\left(H_{3i} - H_{3o}\right) - \left(H_{SC4i} - H_{4o}\right)}{B_x}\right). \tag{5}$$

The experimental slalom test drive was carried out ten times for measurement repeatability. When processing the measured data, we performed a quick check to see if they corresponded to the expected waveforms. After mutual comparison, we verified the test results for the expected waveform. Subsequently, we proceeded to eliminating outliers. If some of the measured waveforms were obviously different, we found the cause and repeated the entire set of experiments. Since we compared two similar sets of measurements, we did not have to recalculate the measured waveforms of the quantities to the centre of gravity of the car.

The measured waveforms of ultrasonic distance sensors (H_{3i}, H_{SC3i}, H_{4i}, H_{SC4i}) and the signals from the longitudinal and lateral acceleration sensors were smoothened by means of a moving average at the time interval $t = 0.2$ s. The distortion of the measured waveform is negligible at this interval. The car turning speed and the slip angle were again smoothened using the moving average at a defined time interval, and then subjected to an off-time correction based on the data obtained from the compensation measurement. The signal from the longitudinal and lateral acceleration sensors was smoothed by means of a moving average at the interval $t = 0.2$ s.

The steering wheel turning angle β_v, the lateral acceleration a_y, the body tilt angle β_i and the position of the right side of the ASC frame H_{SC4i} have positive values in driving the car in a left bend. The turning velocity ω, the slip angle φ, the position of the left side of the ASC frame H_{SC4i} and the car turning angle Ψ have negative values.

3. Results and Discussion

There are values in the waveforms of the measured quantities that are caused by the position of the car due to the car being driven to the experimental measurement at the interval before the car starts, as described above. Above all, the position of the car body is not in the equilibrium position, but in an inclined position. The inclination is caused by the prestressing of rubber parts in the chassis resulting from the car being stopped by the service brake. There is a rapid increase in longitudinal acceleration due to the limited space and short test corridor when starting the experimental vehicle. Subsequently, similar prestressing occurs in the car appendages as when braking, and the body is not in a balanced position. Therefore, we evaluate the measured quantities at the time interval after the car enters the test corridor.

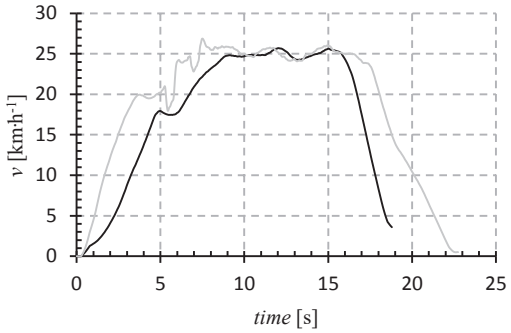

Fig. 6 Driving speed v: – EX; – ASC

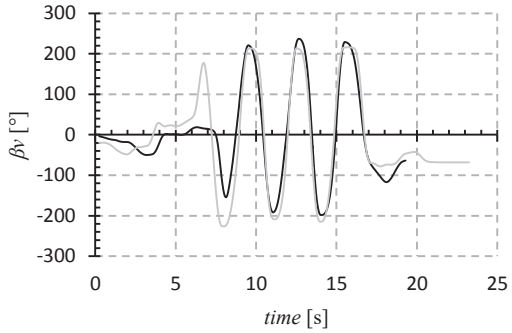

Fig. 7 Steering angle βv: – EX; – ASC

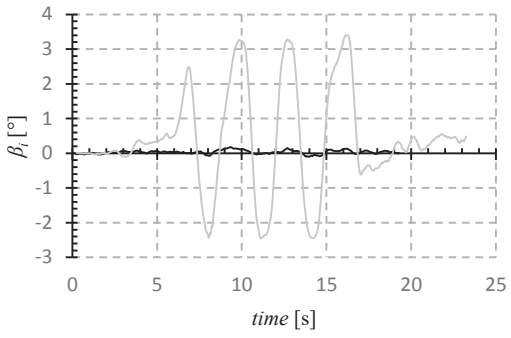

Fig. 8 Tilt angle of the body β_i: – EX; – ASC

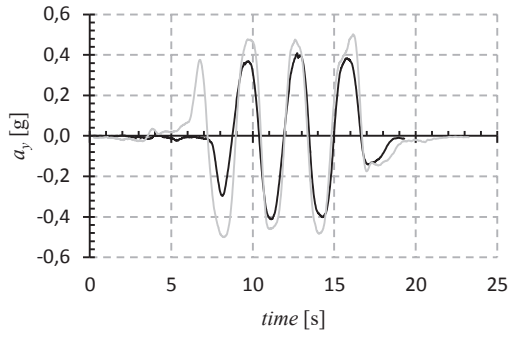

Fig. 9 Lateral acceleration a_y: – EX; – ASC

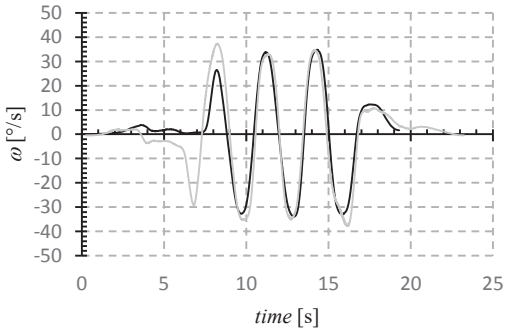

Fig. 10 Turning speed ω: – EX; – ASC

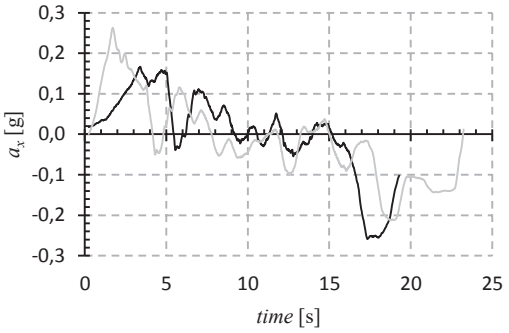

Fig. 11 Longitudinal acceleration a_x: – EX; – ASC

The difference in speed waveforms when driving through the corridor (Fig. 6) is caused by the driver. The driver perceived the speed on a digital instrument cluster located outside their field of vision and thus on the basis of subjective perception. It was necessary to work smoothly with the accelerator pedal so that the car wheels did not slip when starting, even under reduced adhesion conditions. The steering wheel turning angle βv waveform is also determined by the subjective perception of the given corridor by the driver (Fig. 7). Despite the subjective perception of the car's behaviour, the steering wheel turning waveform is comparable in both test drives. It can be seen from the measured waveform of the longitudinal acceleration a_x that the car was not driven at a constant speed during the test drive. The reason for this is that the rolling resistance of the front wheels increases with increasing angles of steering wheel turning lock. Constant speed was kept by correction for accelerator pedal. This applies to both types of test drives.

The body tilt angle βi (Fig. 8) corresponds to the vertical position change values on the sides of the Alternative SkidCar frame. The body tilt is limited by the use of the Alternative SkidCar frame (Fig. 4) and is determined by the tyre stiffness on the ASC wheels (Fig. 3). This significantly limits the car suspension function and the body movement is significantly limited compared to the experimental car on the sliding surface.

The size of the lateral acceleration a_y (Fig. 9) is lower for the ASC than for the experimental car EX. Centrifugal force due to the use of the ASC frame will not cause the body to tilt and thereby overload the outer car wheels. Body tilting moment is captured by the outer wheels of the ASC and the outer car wheels are not overloaded. Due to the use of the ASC frame, the change in radial response on the car wheels caused by driving dynamics is very small compared to the sliding surface. This is why it is easier for the car to skid. The proximity of the skid level is also evident from the mutually analogous waveforms of the steering wheel turning β_v. The same applies to the waveforms of the turning speed ω (Fig. 10). The change in longitudinal acceleration a_x (Fig. 11) is caused by the car moving off before entering the experimental test corridor. It is caused by limited space for experimental measurements.

From the experimentally measured test drive data, it was confirmed that it is possible to reduce the adhesion force transmitted by the car wheels on the road by reducing the weight component on the car wheels with additional wheel units, with unchanged size of the adhesion coefficient. The measured waveforms of typical quantities are similar when comparing the SlideWheel with the sliding surface EX. Significant difference occurs only in the body tilt angle of the experimental car. It is also true for driving on the sliding surface that the car's body tilt decreases as the adhesion force transmitted by the car wheel decreases, and the difference in the body tilt angle between the experimental vehicle and the experimental vehicle with the SW system decreases. To eliminate the subjective influence of the driver, it is possible to use a driving robot in the experimental measurement.

4. Conclusions

The waveforms of the speed v, longitudinal a_x and lateral acceleration a_y in relation to the steering wheel turning angle are comparable in both tests. The biggest differences were achieved when monitoring the body tilt angle. The difference in the body tilt angle corresponds to the waveforms measured by the height sensors. It is true that the body tilt in the alternative SkidCar is negligible compared to the experimental car, and is determined by the stiffness of additional support wheel tyres. The designed Alternative SkidCar system used in the experimental car shown that it can be used to cause a skid at a safe speed of the car; despite the fact that the measured waveforms of the body tilt were different when compared with the sliding surface waveforms. The use of the Alternative SkidCar is possible especially where it is not possible to use the sliding surface or where it is necessary to simulate different adhesion conditions for a particular car wheel. We have been creating a dynamic version of the ASC at the training workplace to make the car's behaviour more natural, particularly by allowing a more intensive tilting of the car body with the change in the lift height of the sprung masses depending on the actual size of the lateral acceleration. In this way, the measured waveforms from the ASC will be even closer to those of the sliding surfaces. More detailed monitoring of ASC system behaviour is subject to further research.

References

1. **Albinsson, A.; Bruzelius, F.; Jacobson, B.** 2018. Evaluation of vehicle-based tyre testing methods, Proceedings of the Institution of Mechanical Engineers Part d-Journal of Automobile Engineering 233: 4-17.
2. **Gao, J.; Zhang, Y.; Du, Y.** 2019. Optimization of the tire ice traction using combined Levenberg Marquardt (LM) algorithm and neural network, Journal of the Brazilian Society of Mechanical Sciences and Engineering 41: 84-96.
3. **Glos, J.; Sejkorová, M.** 2016. Tribo diagnostics as and input for the optimization of vehicles preventive maintenance, Intelligent Technologies in Logistics and Mechatronics Systems, ITELMS 2016–Proccedings of the 11th International Conference, pp. 28-29.
4. **Harun, M.H.; Yunos, M.R.; Md, Azhari, M.A**. 2016. Validation of Vehicle Model Response with an Instrumented Experimental Vehicle, Engineering "Technology International Conference (ETIC) Engineering technology international conference 2016", Ho Chi Minh City, Vietnam, pp. 131-136.
5. **Krmela, J.; Beneš, L.; Krmelová, V.** 2014. Tire experiments on static adhesor for obtaining the radial stiffness value, Period. Polytech, Budapest, Hungary, pp.125-129.
6. **Kulička, J.; Jilek, P.** 2016. The Fourier Analysis in Transport Application Using Matlab. "Transport Means proceedings of the international scientific conference", October 5-7, Kaunas, Lietuva, pp. 820-825.
7. **Lucet, E.; Lenain, R.; Grand, Ch.** 2015. Dynamic path tracking control of a vehicle on slippery terrain, Control engineering practice 42: 60-73.
8. **Marek, V.; Čupera, J.** 2016. Data Mining of Vehicle Control Units. "Proceedings of International PhD Students Conference", 23: 944-948.
9. **Rievaj, V.; Vrabel, J.; Synak, F. etc.** 2018. The effects of vehicle load on driving characteristics, Advances in Science and Technology-Research Journal, 12: 142-149.
10. **Sejkorová, M.; Hurtová, I.; Glos, J.; Pokorný, J.** 2017. Definition of a motor oil change interval for high volume diesel engines based on its current characteristics assessment. Acta Universitatis Agriculturae et Silviculturae Mendelianae Brunensis 65(2): 481-490.
11. **Šarkan, B.; Skrúcaný, T.; Semanová, Š**. etc. 2018. Vehicle coast-down method as a tool for calculating total resistance for the purposes of type-approval fuel consumption. "Scientific Journal of Silesian University of Technology. Series Transport", 98: 161-172.
12. **Verner, J.; Sejkorová, M.** 2018. Comparison of CVS and PEMS measuring devices used for stating CO2 exhaust emissions of light-duty vehicles during WLTP testing procedure. "Engineering for Rural Development", pp. 2054-2059.